

Pair density wave characterized by a hidden string order parameter

Hao-Kai Zhang,¹ Rong-Yang Sun,^{2,3} and Zheng-Yu Weng¹

¹*Institute for Advanced Study, Tsinghua University, Beijing 100084, China*

²*Computational Materials Science Research Team,*

RIKEN Center for Computational Science (R-CCS), Kobe, Hyogo 650-0047, Japan

³*Quantum Computational Science Research Team,*

RIKEN Center for Quantum Computing (RQC), Wako, Saitama 351-0198, Japan

(Dated: December 14, 2022)

A composite pairing structure of superconducting state is revealed by density matrix renormalization group study in a two-leg t - J model. The pairing order parameter is composed of a pairing amplitude and a phase factor, in which the latter explicitly depends on the spin background with an analytic form identified in the anisotropic limit as the interchain hopping integral $t_{\perp} \rightarrow 0$. Such a string-like phase factor is responsible for a pair density wave (PDW) induced by spin polarization with a wavevector $Q_{\text{PDW}} = 2\pi m$ (m the magnetization). By contrast, the pairing amplitude remains smooth, unchanged by the PDW. In particular, a local spin polarization can give rise to a sign change of the order parameter across the local defect. Unlike in an Fulde-Ferrell-Larkin-Ovchinnikov state, the nonlocal phase factor here plays a role as the new order parameter characterizing the PDW, whose origin can be traced back to the essential sign structure of the doped Mott insulator.

Introduction.— Pair density wave (PDW) states are superconducting (SC) states in which Cooper pairs have a finite center-of-mass momentum so that the SC order parameter oscillates spatially with vanishing average [1]. Such states have been studied to understand cuprate superconductors especially for the dynamical inter-layer decoupling phenomena [2–5]. Signatures of PDW states have also been reported via local Cooper pair tunneling and scanning tunneling microscopy [6–8]. In weak correlated systems, the Fulde-Ferrell-Larkin-Ovchinnikov (FFLO) state [9, 10] is the first example of PDW states based on the BCS theory where the Fermi surfaces of different spins are split by the Zeeman field. By contrast, in strongly correlated systems such as doped Mott insulators where the standard BCS picture may not generally hold, the mechanism for PDW is still under debate in either the presence or absence of an external magnetic field [11–21].

To explore the mechanism of superconductivity in a doped Mott insulator, a two-leg t - J ladder may serve as an interesting toy model [22–26], in which a quasi-one-dimensional SC state or the Luther-Emery (LE) liquid [27] has been previously established, with a strong pairing of doped holes in a short-range antiferromagnetic (AFM) spin background. In particular, the LE phase remains robust and can be smoothly extrapolated to the limit of the inter-chain hopping integral $t_{\perp} = 0$ [24]. In the latter, an analytic composite pairing structure can be identified, where the pairing amplitude and phase is explicitly separated to describe the pairing of the “twisted” doped holes and a nonlocal spin-dependent phase shift, respectively [24, 28, 29]. It suggests that SC phase coherence may be critically examined by fine-tuning the spin background without destroying the pairing at a given doping concentration.

In this paper, we employ the density matrix renormal-

ization group (DMRG) method [30] to study the ground state of the doped t - J two-leg ladder by polarizing the background spins. It is shown that the pairing remains robust beyond the LE phase to persist into a PDW state once a uniform spin magnetization (m) sets in, resulting in an algebraic-decaying SC correlator oscillating in sign spatially. In particular, the pairing order parameter can change sign even across locally polarized spins, indicating a non-FFLO type of mechanism. The hole pairing eventually vanishes and a Fermi liquid (FL) occurs as schematically summarized in Fig. 1. In the limit of $t_{\perp} \rightarrow 0$, an analytic form enables an explicit separation of a pairing amplitude from a string-like phase factor, which plays a role of an order parameter to solely determine the PDW wavevector $Q_{\text{PDW}} = 2\pi m$. Finally it is argued generally that the PDW is a direct manifestation of the phase-string sign structure in the model, and the PDW disappears in the whole phase diagram once the phase-string is turned off in the DMRG simulation.

Model and method.— The basic physics of doped Mott insulators in the strong coupling limit is described by the standard t - J model with Hamiltonian $H_{t-J} = \mathcal{P}_s (H_t + H_J) \mathcal{P}_s$, where

$$\begin{aligned} H_t &= - \sum_{\langle ij \rangle \sigma} t_{ij} \left(c_{i\sigma}^{\dagger} c_{j\sigma} + h.c. \right), \\ H_J &= \sum_{\langle ij \rangle} J_{ij} \left(\mathbf{S}_i \cdot \mathbf{S}_j - \frac{1}{4} n_i n_j \right). \end{aligned} \quad (1)$$

Here $c_{i\sigma}$ is the electron annihilation operator on lattice site $i = (x, y)$ with spin index $\sigma \in \{\uparrow, \downarrow\}$. \mathbf{S}_i and n_i are the spin and electron number operators, respectively. The Hilbert space is constrained by the no-double-occupancy condition $n_i = \sum_{\sigma} n_{i\sigma} = \sum_{\sigma} c_{i\sigma}^{\dagger} c_{i\sigma} \leq 1$ on each site imposed by the projector \mathcal{P}_s . t_{ij} is the hopping integral and J_{ij} is the superexchange coupling between

the nearest-neighbor (NN) sites $\langle ij \rangle$ on a square lattice of size $N = L_x \times L_y$. We fix $J_{ij} = J = 1$ as the energy unit and $t = 3$ along the \hat{x} -direction. The interchain hopping integral along the \hat{y} -direction is set to be $t_{ij} = t_\perp$ as an adjustable parameter. To polarize the background spins, we apply a uniform Zeeman field via $H_h = -hS^z$, where $S^z = \sum_i S_i^z$ denotes the total spin z -component. Here we focus on two-leg ladders $L_y = 2$ with length L_x up to 192 and hole doping at $\delta = N_h/N = 1/8$ where N_h denotes the number of doped holes. We perform 50-200 sweeps and keep the bond dimension up to 15000 with a typical truncation error $\epsilon \lesssim 10^{-8}$. The simulations are based on the GraceQ project [32].

Phase diagram.— Three distinct phases are identified for the two-leg t - J ladder at finite doping by tuning the spin polarization $m \equiv \langle S^z \rangle / N$ via the Zeeman field h (see Fig. 1). At $m = 0$, the ground state is a robust LE liquid with a quasi-long-range SC order in the whole region of $0 \leq t_\perp/t \leq 1$ [24]. A phase transition occurs at $m \neq 0$ to a PDW phase, which is characterized by an algebraic-decaying SC correlation that oscillates in sign (see below). Eventually a Fermi liquid (FL) phase sets in, which can be continuously extrapolated to the spin fully polarized limit. A phase separation (PS) region lies between the PDW and FL phases, which are distinguished by the pairing and non-pairing of the doped holes.

The magnetization m is shown in Fig. 2(a) and (b) together with the static susceptibility $\chi = \frac{\partial m}{\partial h}$ at $t_\perp/t = 1$ and $t_\perp = 0$, respectively. The LE/PDW phase boundary is at the onset of m (cf. the sharp peak of χ on the weak field side) where the Zeeman energy equals to the

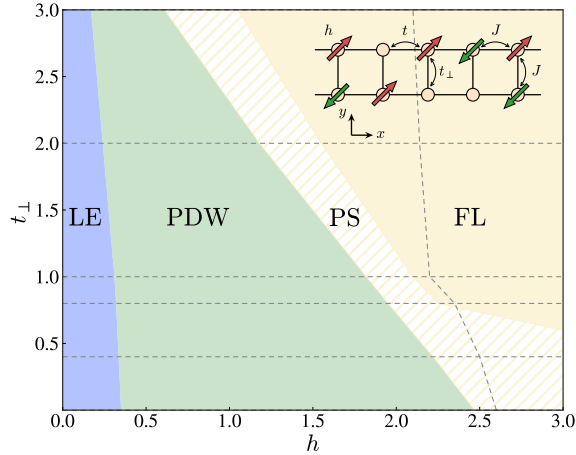


FIG. 1. Ground state phase diagram of two-leg t - J ladder (see the inset) at $t/J = 3$ and $\delta = 1/8$ with respect to the Zeeman field h and the interchain hopping t_\perp in units of J . The three colored regions are identified as the LE, PDW and FL phases, with the shaded area as the phase separation (PS) region. The horizontal and vertical dashed lines mark the swept parameter points and the magnetization saturation, respectively [31].

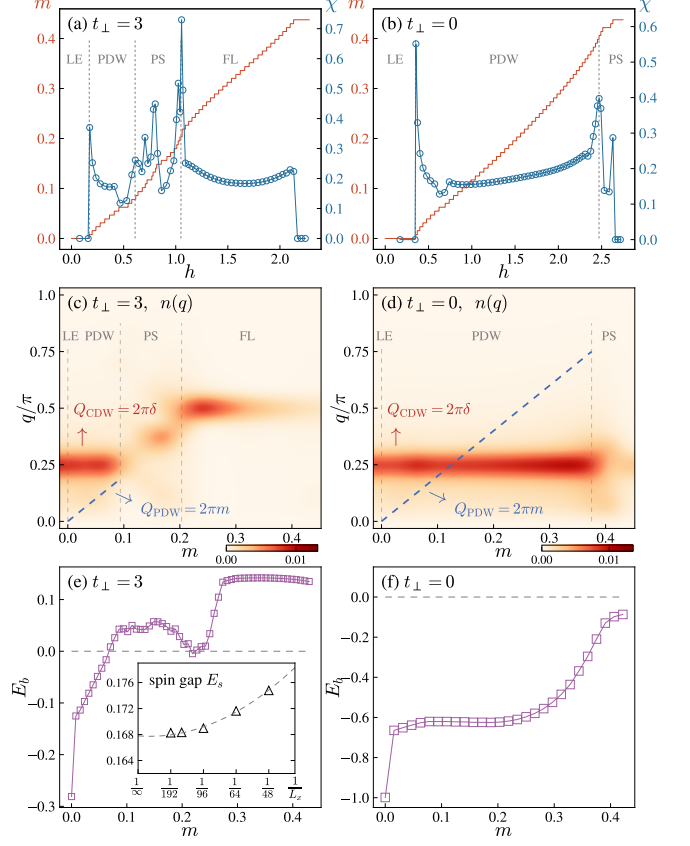


FIG. 2. (a) and (b): Magnetization m and static susceptibility χ versus the Zeeman field h for the isotropic limit $t_\perp = 3$ and anisotropic limit $t_\perp = 0$ of a two-leg t - J ladder with $L_x = 64$ at $\delta = 1/8$. (c) and (d): Fourier spectrum $n(q)$ of the charge density versus m . The CDW wavevector Q_{CDW} and PDW wavevector Q_{PDW} are independent from each other in the LE and PDW phases. (e) and (f): Binding energy E_b of two doped holes as a function of m (with $L_x = 64, 32$), where negative values of E_b indicate the existence of pairing. The inset in (e) depicts the finite-size scaling of the spin gap E_s for the isotropic case.

spin gap: i.e., $h\langle S^z \rangle = E_s$, with E_s shown in the inset of Fig. 2(e) which is defined by

$$E_s(N_h) = E(N_h, S^z = 1) - E(N_h, S^z = 0). \quad (2)$$

Here $E(N_h, S^z)$ denotes the ground state energy with the fixed number of doped holes N_h and the total spin S^z .

The LE phase has a CDW or charge density modulation at wavevector $Q_{\text{CDW}} = 2\pi\delta$ [24], which persists over to the whole PDW phase as indicated in Fig. 2(c) and (d). Here the charge density distribution along the \hat{x} -direction is defined by $n(x) = \sum_{y=1}^{L_y} \langle n_{x,y} \rangle / L_y$ with the Fourier transformation $n(q) = |\sum_x n(x) e^{iqx}| / R$ (here x is summed over the central bulk of length $R = L_x/2$ to reduce the boundary effect).

In sharp contrast, Q_{CDW} is independent of the PDW wavevector at $Q_{\text{PDW}} = 2\pi m$ (see below). Both of which

disappear simultaneously at the boundary of the phase separation, indicated in Figs. 2(c) and (d), where the density profile becomes spatially inhomogeneous like a mixture of the PDW and FL regimes on the both sides. One is referred to Fig. S1 of the Supplemental Material [31] for more details.

Furthermore, the hole pairing can be determined by computing the binding energy

$$E_b(N_h, S^z) \equiv E(N_h + 2, S^z) + E(N_h, S^z) - E(N_h + 1, S^z + \frac{1}{2}) - E(N_h + 1, S^z - \frac{1}{2}). \quad (3)$$

As shown in Figs. 2(e) and (f), E_b is negative in both the LE and PDW phases, which then vanishes and becomes positive in the phase separation and FL regions.

PDW and composite pairing structure.— The PDW phase has been previously conjectured to be an FFLO-like state in the isotropic limit [23]. Nevertheless, the independence of Q_{CDW} and Q_{PDW} [cf. Fig. 2(c) and (d)] strongly suggest that both orders may not be originated from a naive spin-polarized Fermi surface effect. According to the phase diagram, the LE and PDW phases can continuously persist over the whole region of $0 \leq t_{\perp}/t \leq 1$, and in particular, the PDW is most robust against a finite m at $t_{\perp} = 0$ in Fig. 1. In the following, we shall first focus on the PDW state in the anisotropic limit of $t_{\perp} = 0$, where some precise and useful analytic structure is available [28, 29].

Here the pairing order parameter may be explicitly decomposed into the amplitude and phase components [28, 29] in a form $\langle \Delta_x \rangle \propto \langle \tilde{\Delta}_x \rangle \langle e^{i\phi_x} \rangle$. Specifically, the spin-singlet pair operator $\Delta_x \equiv \frac{1}{\sqrt{2}} \sum_{\sigma} \sigma c_{x1,\sigma} c_{x2,-\sigma}$, which is defined at the rung of sites $(x, 1)$ and $(x, 2)$, may be rewritten as [31]

$$\Delta_x = \frac{1}{\sqrt{2}} \left(\tilde{c}_{x1,\uparrow} \tilde{c}_{x2,\downarrow} e^{i(\Omega_{x1,\downarrow} + \Omega_{x2,\uparrow})} - \tilde{c}_{x1,\downarrow} \tilde{c}_{x2,\uparrow} e^{i(\Omega_{x1,\uparrow} + \Omega_{x2,\downarrow})} \right), \quad (4)$$

where the “twisted” holes are defined by $\tilde{c}_{i,\sigma} = c_{i,\sigma} e^{-i\Omega_{i,-\sigma}}$, with the string operator $\Omega_{xy,\sigma} \equiv \pi \sum_{x' > x} n_{x',y,\sigma}$ in which the summation runs over one of the 1D chains of the two-leg ladder. Define the pairing amplitude $\tilde{\Delta}_x \equiv \frac{1}{\sqrt{2}} \sum_{\sigma} \sigma \tilde{c}_{x1,\sigma} \tilde{c}_{x2,-\sigma}$ and the string-like phase $\phi_x \equiv \Omega_{x1,\downarrow} + \Omega_{x2,\uparrow}$ [31]. Correspondingly, the pair-pair correlators of $P(r) = \langle \Delta_{x_0}^{\dagger} \Delta_{x_0+r} \rangle$, as well as the sub-components $\tilde{P}(r) = \langle \tilde{\Delta}_{x_0}^{\dagger} \tilde{\Delta}_{x_0+r} \rangle$ and $\Phi(r) = \langle e^{-i\phi_{x_0}} e^{i\phi_{x_0+r}} \rangle$ can be computed separately. The results including their Fourier transformations are presented in Fig. 4 (here the rung at $x_0 = L_x/4$ is set as a reference bond and the distance r is between two rungs).

At $m = 0$, the two pair-pair correlators, $P(r)$ and $\tilde{P}(r)$, are essentially the same [28] as shown in Fig. 3(a) and (c), which is due to the fact that the phase fluctuation of the phase ϕ_x gets cancelled out by the short-range AFM

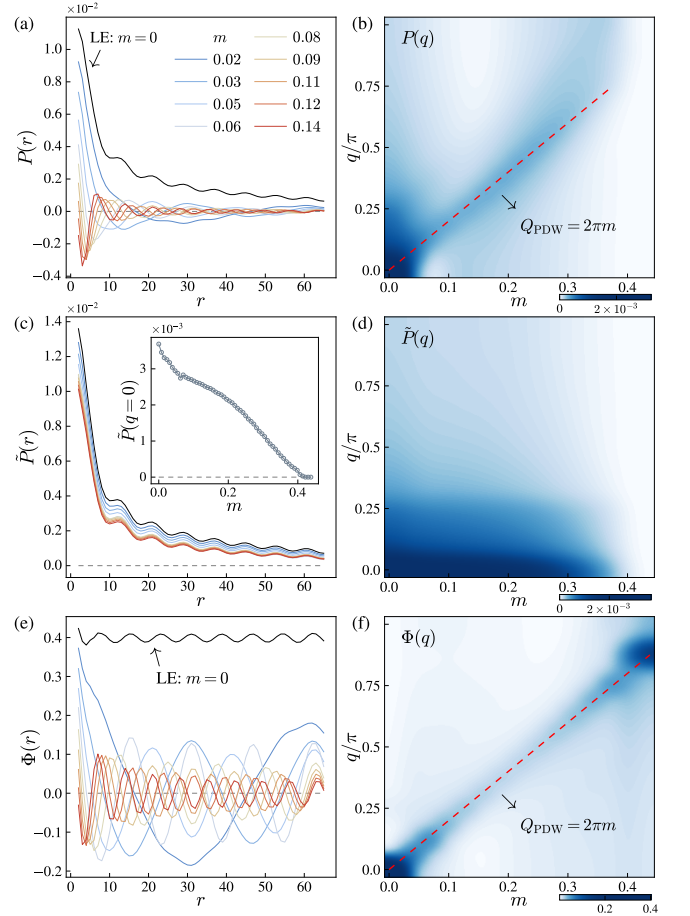


FIG. 3. Composite structure of the pairing order parameter at $t_{\perp} = 0$ ($\delta = 1/8$). (a) and (b): Pair-pair correlator in the real space ($L_x = 128$) and momentum space ($L_x = 64$) versus m , respectively. (c) and (d): The corresponding correlator of the pairing amplitude (see text). The inset in (c) depicts the overall magnitude of $\tilde{P}(r)$ as a function of m . (e) and (f): The corresponding correlator of the phase component of the pairing order parameter in the real and momentum space.

correlation. But once $m \neq 0$, $P(r)$ exhibits a PDW oscillation at a *new* wavevector $Q_{\text{PDW}} = 2\pi m$ [Fig. 3(a) and (b)] with a polynomial-decaying envelope. By contrast, $\tilde{P}(r)$ still behaves the same as in the LE ($m = 0$) phase such that the PDW oscillation entirely comes from the phase factor as shown by $\Phi(r)$ in Fig. 3(e) and (f). The DMRG results shown in Fig. 3 confirm that the SC order parameter can be indeed decomposed into an amplitude $\tilde{\Delta}_x$ and a phase factor $e^{i\phi_x}$, respectively, which behave independently in the $t_{\perp} = 0$ limit. Namely, the amplitude component will characterize the preformed hole pairs in both the LE and PDW phases, with $\tilde{P}(r)$ only smoothly reducing with the increase of m . On the other hand, the string-like phase factor changes qualitatively from a constant at $m = 0$ (with a weak CDW ingredient) to a predominant PDW oscillation at $m \neq 0$ in Fig. 3(c). In other words, such a string-like phase factor can serve

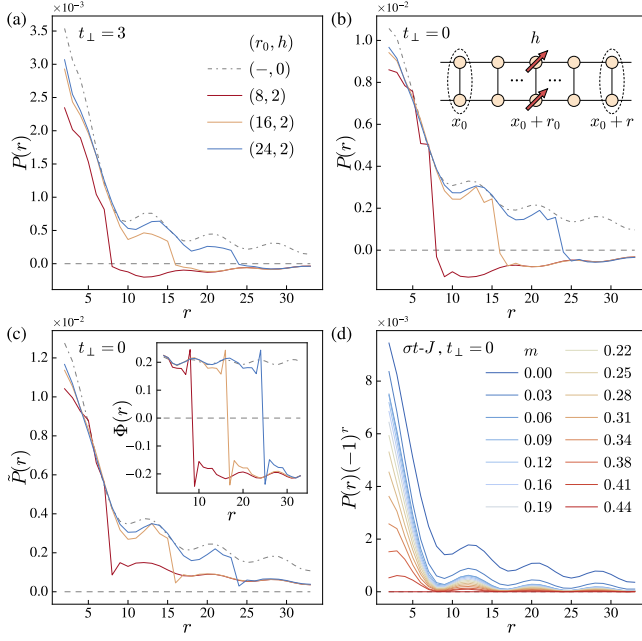


FIG. 4. Pair-pair correlator at $t_{\perp} = 3$ (a) and $t_{\perp} = 0$ (b), respectively, shows a sign change across the local spin polarizations at rung $x_0 + r_0$, which are induced by a strong local Zeeman field as indicated in the inset of (b). (c) The composite pairing structure: the phase-shift operator (the inset) is responsible for the sign change of the pair-pair correlator, while the pairing amplitude is unchanged in sign across the local “defect”. (d) By turning off the phase-string in the t - J ladder (see text), the pair-pair correlator no longer exhibits any additional “PDW” order at a finite m ($L_x = 64$).

as the *sole* PDW order parameter. As a matter of fact, it is clearly shown in Figs. S3 and S4 of the Supplemental Material [31], that the product of $\tilde{P}(r)$ and $\Phi(r)$ can very precisely reproduce the curve of $P(r)$ except for an overall numerical factor, which means that the composite pairing structure $\langle \Delta_x \rangle \propto \langle \tilde{\Delta}_x \rangle \langle e^{i\phi_x} \rangle$ or the separation of the pairing amplitude (charge) and the phase (spin) is indeed highly accurate in the sense of a generalized mean-field description. A generalization to the two-dimensional isotropic case has been made recently for two holes [33].

It is important to note that beyond a uniform Zeeman field, a local spin polarization in the background may also lead to a nonlocal phase change in the SC order parameter via $e^{i\phi_x}$. To test this effect, one may apply a strong local Zeeman field to polarize the spins in a given rung at $x_0 + r_0$ [cf. the inset of Fig. 4(b)] which indeed leads to the sign changes of the SC correlator between rung x_0 and r across the defect at $x_0 + r_0$ for $t_{\perp} = 3$ (isotropic case) and $t_{\perp} = 0$, respectively, as illustrated in Fig. 4(a) and (b) at different r_0 's. In particular, the corresponding pairing amplitude correlator $\tilde{P}(r)$ remains positive-definite, while $\Phi(r)$ changes sign across the defect, which are illustrated in Fig. 4(c) at $t_{\perp} = 0$.

Physical origin of PDW.— We have so far identified

a novel entanglement between the Cooper pair and the background spins that can lead to a PDW order via spin polarization. In the following, we give a general physical argument on the origin of such a PDW based on a fundamental property of the doped Mott insulator. We note that the partition function of the t - J model can be in general expressed as $Z_{t-J} = \sum_c \tau_c W[c]$ with $W[c] \geq 0$ and $\tau_c = (-1)^{N_{\downarrow}^h[c]} (-1)^{N_{\text{ex}}^h[c]}$ where c represents the closed loops of all the spins and holes [34]. Here $(-1)^{N_{\text{ex}}^h[c]}$ represents a conventional fermionic sign structure for the doped holes like in a doped semiconductor, but $(-1)^{N_{\downarrow}^h[c]}$ is unique for a doped Mott insulator, which depends on the parity of the number of *mutual exchanges* between holes and \downarrow -spins, known as the phase-string. Noting that $N_{\downarrow}^h = (N_{\uparrow}^h + N_{\downarrow}^h)/2 + (N_{\uparrow}^h - N_{\downarrow}^h)/2$. Then it is easy to see that the second term can contribute to a nontrivial spin-polarization-dependent phase factor $\exp[\pm i\pi \sum_{i \in c} S_i^z]$ associated with each hole path. Accordingly for a pair of holes traversing along the \hat{x} -direction of the two-leg ladder, by a distance L_{AB} , the pair-pair correlators will generally acquire an additional phase factor $\exp[\pm i2\pi \langle S_{AB}^z \rangle]$, which gives rise to the PDW wavevector Q_{PDW} by noting that $\langle S_{AB}^z \rangle = mL_{AB}$ for a uniform m , or the sign change in the SC order parameter across a sufficiently large local spin polarization [cf. Figs. 4(a)-(c)]. Finally, the phase-string factor in τ_c can be precisely switched off, without changing $W[c]$ in Z_{t-J} , by inserting a spin-dependent sign σ in the hopping term $H_{\sigma t} = -\sum_{\langle ij \rangle \sigma} \sigma t_{ij} c_{i\sigma}^{\dagger} c_{j\sigma} + h.c.$, which results in the so-called $\sigma \cdot t$ - J model [35]. Then carrying out the similar DMRG calculation, one finds that the PDW is no longer present at $m \neq 0$ as shown in Fig. 4(d).

In conclusion, a Cooper pair moving on a spin-polarized background can acquire a new oscillating phase, which illustrates a general mutual entanglement between the doped charge and spin degrees of freedom in the t - J model. In contrast to a conventional FFLO state in the BCS theory, the doped holes here are drastically “twisted” by the underlying phase-string effect, as explicitly shown in the $t_{\perp} = 0$ case, which can result in strongly preformed pairing of holes that is not sensitive to the Zeeman field. However, the phase coherence of the hole pair is further tied to the singlet or resonating-valence-bond pairing of spins. Once the latter is broken by a partial polarization, the pairing order parameter is fundamentally changed to lead to a PDW state. Along this line, a further investigation into the phase of the pairing order parameter by tuning the spin background [25] may reveal more underlying novel structure of a doped Mott insulator.

Acknowledgments.— Stimulating discussions with Jia-Xin Zhang, Jing-Yu Zhao, and Zheng Zhu are acknowledged. This work is partially supported by MOST of China (Grant No. 2021YFA1402101).

-
- [1] Daniel F Agterberg, J. C. Séamus Davis, Stephen D Edkins, Eduardo Fradkin, Dale J. Van Harlingen, Steven A Kivelson, Patrick A Lee, Leo Radzihovsky, John M Tranquada, and Yuxuan Wang, “The Physics of Pair-Density Waves: Cuprate Superconductors and beyond,” (2020) and reference therein.
- [2] A. Himeda, T. Kato, and M. Ogata, “Stripe States with Spatially Oscillating d -Wave Superconductivity in the Two-Dimensional t - t' - J Model,” *Physical Review Letters* **88**, 117001 (2002).
- [3] Q. Li, M. Hücker, G D Gu, A M Tsvelik, and J M Tranquada, “Two-dimensional superconducting fluctuations in stripe-ordered $\text{La}_{1.875}\text{Ba}_{0.125}\text{CuO}_4$,” *Physical Review Letters* **99**, 4–7 (2007), [arXiv:0703357 \[cond-mat\]](#).
- [4] E. Berg, E. Fradkin, E.-A. Kim, S. A. Kivelson, V. Oganesyan, J. M. Tranquada, and S. C. Zhang, “Dynamical Layer Decoupling in a Stripe-Ordered High- T_c Superconductor,” *Physical Review Letters* **99**, 127003 (2007), [arXiv:0704.1240](#).
- [5] P. M. Lozano, Tianhao Ren, G. D. Gu, A. M. Tsvelik, J. M. Tranquada, and Qiang Li, “Testing for pair density wave order in $\text{La}_{1.875}\text{Ba}_{0.125}\text{CuO}_4$,” *Physical Review B* **106**, 174510 (2022), [arXiv:2110.05513](#).
- [6] M. H. Hamidian, S. D. Edkins, Sang Hyun Joo, A. Kostin, H. Eisaki, S. Uchida, M. J. Lawler, E.-A. Kim, A. P. Mackenzie, K. Fujita, Jinho Lee, and J. C. Séamus Davis, “Detection of a Cooper-pair density wave in $\text{Bi}_2\text{Sr}_2\text{CaCu}_2\text{O}_{8+x}$,” *Nature* **532**, 343–347 (2016), [arXiv:1511.08124](#).
- [7] Wei Ruan, Xintong Li, Cheng Hu, Zhenqi Hao, Haiwei Li, Peng Cai, Xingjiang Zhou, Dung Hai Lee, and Yayu Wang, “Visualization of the periodic modulation of Cooper pairing in a cuprate superconductor,” (2018).
- [8] S D Edkins, A Kostin, K Fujita, A P Mackenzie, H Eisaki, S Uchida, Subir Sachdev, Michael J Lawler, E. A. Kim, J. C. Séamus Davis, and M H Hamidian, “Magnetic field-induced pair density wave state in the cuprate vortex halo,” *Science* **364**, 976–980 (2019), [arXiv:1802.04673](#).
- [9] Peter Fulde and Richard A. Ferrell, “Superconductivity in a Strong Spin-Exchange Field,” *Physical Review* **135**, A550–A563 (1964).
- [10] A. I. Larkin and Y. N. Ovchinnikov, “Nonuniform state of superconductors,” *Soviet Physics-JETP* **20**, 762–770 (1965).
- [11] Erez Berg, Eduardo Fradkin, Steven A. Kivelson, and John M. Tranquada, “Striped superconductors: how spin, charge and superconducting orders intertwine in the cuprates,” *New Journal of Physics* **11**, 115004 (2009).
- [12] Erez Berg, Eduardo Fradkin, and Steven A. Kivelson, “Pair-density-wave correlations in the Kondo-Heisenberg model,” *Physical Review Letters* **105**, 2–5 (2010).
- [13] Florian Loder, Arno P. Kampf, and Thilo Kopp, “Superconducting state with a finite-momentum pairing mechanism in zero external magnetic field,” *Physical Review B* **81**, 020511 (2010).
- [14] Florian Loder, Siegfried Graser, Arno P. Kampf, and Thilo Kopp, “Mean-field pairing theory for the charge-stripe phase of high-temperature cuprate superconductors,” *Physical Review Letters* **107**, 1–4 (2011).
- [15] Patrick A. Lee, “Amperean Pairing and the Pseudogap Phase of Cuprate Superconductors,” *Physical Review X* **4**, 031017 (2014), [arXiv:1401.0519](#).
- [16] Jonatan Wårdh and Mats Granath, “Effective model for a supercurrent in a pair-density wave,” *Physical Review B* **96**, 1–11 (2017), [arXiv:1703.03781](#).
- [17] Jonatan Wårdh, Brian M. Andersen, and Mats Granath, “Suppression of superfluid stiffness near a Lifshitz-point instability to finite-momentum superconductivity,” *Physical Review B* **98**, 1–10 (2018), [arXiv:1807.05303](#).
- [18] Chandan Setty, Laura Fanfarillo, and P. J. Hirschfeld, “Microscopic mechanism for fluctuating pair density wave,” , 1–13 (2021), [arXiv:2110.13138](#).
- [19] Chandan Setty, Jinchao Zhao, Laura Fanfarillo, Edwin W. Huang, Peter J. Hirschfeld, Philip W. Phillips, and Kun Yang, “Exact solution for finite center-of-mass momentum Cooper pairing,” (2022), [arXiv:2209.10568](#).
- [20] Hong-Chen Jiang, “Pair density wave in doped three-band Hubbard model on square lattice,” (2022), [arXiv:2209.11381](#).
- [21] Yi-Ming Wu, P. A. Nosov, Aavishkar A. Patel, and S. Raghu, “Pair density wave order from electron repulsion,” (2022), [arXiv:2209.09254](#).
- [22] D. Poilblanc, D. J. Scalapino, and W. Hanke, “Spin and charge modes of the t - J ladder,” *Physical Review B* **52**, 6796–6800 (1995).
- [23] G. Roux, S. R. White, S. Capponi, and D. Poilblanc, “Zeeman effect in superconducting two-leg ladders: Irrational magnetization plateaus and exceeding the Pauli limit,” *Physical Review Letters* **97**, 1–4 (2006), [arXiv:0512025 \[cond-mat\]](#).
- [24] Hong-Chen Jiang, Shuai Chen, and Zheng-Yu Weng, “Critical role of the sign structure in the doped Mott insulator: Luther-Emery versus Fermi-liquid-like state in quasi-one-dimensional ladders,” *Physical Review B* **102**, 104512 (2020).
- [25] Rong-Yang Sun, Zheng Zhu, and Zheng-Yu Weng, “Complex phase diagram of doped XXZ ladder: Localization and pairing,” *Physical Review Research* **2**, 033007 (2020), [arXiv:2002.03529](#).
- [26] Kazuya Shinjo, Shigetoshi Sota, and Takami Tohyama, “Effect of phase string on single-hole dynamics in the two-leg Hubbard ladder,” *Physical Review B* **103**, 035141 (2021), [arXiv:2011.10686](#).
- [27] A. Luther and V. J. Emery, “Backward Scattering in the One-Dimensional Electron Gas,” *Physical Review Letters* **33** (1974), 10.1103/PhysRevLett.33.589.
- [28] Zheng Zhu, D N Sheng, and Zheng Yu Weng, “Pairing versus phase coherence of doped holes in distinct quantum spin backgrounds,” *Physical Review B* **97**, 1–8 (2018), [arXiv:1706.02305](#).
- [29] Shuai Chen, Zheng Zhu, and Zheng-Yu Weng, “Two-hole ground state wavefunction: Non-BCS pairing in a t - J two-leg ladder,” *Physical Review B* **98**, 245138 (2018), [arXiv:1808.06173](#).
- [30] Steven R. White, “Density matrix formulation for quantum renormalization groups,” *Physical Review Letters* **69** (1992), 10.1103/PhysRevLett.69.2863.
- [31] See Supplemental Material for more data analyses supporting the phase diagram and the conclusion on the pairing amplitude and phase.
- [32] GraceQ, [www.gracequantum.org](#).
- [33] Jing Yu Zhao, Shuai A Chen, Hao Kai Zhang, and Zheng Yu Weng, “Two-Hole Ground State: Dichotomy in Pairing Symmetry,” *Physical Review X* **12**, 1–22 (2022), [arXiv:2106.14898](#).

- [34] K Wu, Z Y Weng, and J Zaanen, “Sign structure of the t - J model,” [Physical Review B - Condensed Matter and Materials Physics](#) **77**, 1–5 (2008).
- [35] Zheng Zhu, Hong Chen Jiang, Yang Qi, Chu-Shun Tian, and Zheng Yu Weng, “Strong correlation induced charge localization in antiferromagnets,” [Scientific Reports](#) **3** (2013), 10.1038/srep02586, [arXiv:1212.6634](#).
- [36] D N Sheng, Y C Chen, and Z Y Weng, “Phase string effect in a doped antiferromagnet,” [Physical Review Letters](#) **77**, 5102–5105 (1996).
- [37] Z. Y. Weng, D. N. Sheng, Y.-C. Chen, and C. S. Ting, “Phase string effect in the t - J model: General theory,” [Physical Review B](#) **55**, 3894–3906 (1997).
- [38] Zheng Yu Weng, “Superconducting ground state of a doped Mott insulator,” [New Journal of Physics](#) **13** (2011), 10.1088/1367-2630/13/10/103039.

Supplemental Material for “Pair density wave characterized by a hidden string order parameter”

This supplemental material contains more numerical results and detailed analyses to further support the conclusions we have discussed in the main text. We first introduce the general definition of the twisted quasiparticle. Then we show more data on density profiles and technical details to support the proposed phase diagram. Finally we provide more information on correlation functions and careful analyses on the composite structure of the pair-pair correlators.

1. Definition of the twisted quasiparticle

We show a simple derivation of the definition of the twisted quasiparticle $\tilde{c}_{i\sigma}$ presented in the main text. Inspired by the mutual statistics between spin and hole in the t - J model due to the phase-string sign structure [34, 36, 37], we perform the following duality transformation [38]

$$e^{i\Theta} = \exp \left(-i \sum_{i \neq j} n_i^h n_{j\downarrow} \theta_{ij} \right) = \exp \left(-i \sum_i n_i^h \Omega_{i\downarrow} \right), \quad (S1)$$

where $\Omega_{i\downarrow} = \sum_{j \neq i} n_{j\downarrow} \theta_{ij}$ counts the statistical phase contributed from the \downarrow -spins around site i and $\theta_{ij} = \text{Im} \ln(z_i - z_j)$ denotes the statistical angle between site i to site j with $z_i = x_i + iy_i$ being the complex coordinate. Then the transformed (or twisted) fermion operator is

$$\tilde{c}_{i\sigma} = e^{i\Theta} c_{i\sigma} e^{-i\Theta} = e^{-i \sum_{j \neq i} (n_i^h n_{j\downarrow} \theta_{ij} + n_j^h n_{i\downarrow} \theta_{ji})} c_{i\sigma} e^{i \sum_{j \neq i} (n_i^h n_{j\downarrow} \theta_{ij} + n_j^h n_{i\downarrow} \theta_{ji})}. \quad (S2)$$

For different spin orientations, we have

$$\begin{aligned} \tilde{c}_{i\uparrow} &= e^{-i \sum_{j \neq i} n_i^h n_{j\downarrow} \theta_{ij}} c_{i\uparrow} = c_{i\uparrow} e^{-i \sum_{j \neq i} n_{j\downarrow} \theta_{ij}} = c_{i\uparrow} e^{-i \Omega_{i\downarrow}}, \\ \tilde{c}_{i\downarrow} &= e^{-i \sum_{j \neq i} n_i^h n_{j\downarrow} \theta_{ij}} c_{i\downarrow} e^{i \sum_{j \neq i} n_j^h n_{i\downarrow} \theta_{ji}} = c_{i\downarrow} e^{-i \sum_{j \neq i} (n_{j\downarrow} \theta_{ij} - n_j^h \theta_{ji})} = c_{i\downarrow} e^{-i(\Omega_{i\downarrow} + \Phi_i^h)} (-1)^{\hat{N}_h}. \end{aligned} \quad (S3)$$

where $\Phi_i^h = \sum_{j \neq i} n_j^h \theta_{ij}$. The constant term $(-1)^{\hat{N}_h}$ can be omitted. According to the no-double-occupancy constraint $n_{i\uparrow} + n_{i\downarrow} + n_i^h = 1$, we have $\Phi_i^h = \Phi_i^0 - \Omega_{i\uparrow} - \Omega_{i\downarrow}$, where $\Phi_i^0 = \sum_{j \neq i} \theta_{ij}$ and $\Omega_{i\uparrow} = \sum_{j \neq i} n_{j\uparrow} \theta_{ij}$. Substitute this relation into Eq. (S3) and we obtain

$$\tilde{c}_{i\uparrow} = c_{i\uparrow} e^{-i \Omega_{i\downarrow}}, \quad \tilde{c}_{i\downarrow} = c_{i\downarrow} e^{-i(\Phi_i^0 - \Omega_{i\uparrow})}. \quad (S4)$$

The Φ_i^0 term which contributes a trivial 2π winding flux can be omitted. Finally, we arrive at $\tilde{c}_{i\sigma} = c_{i\sigma} e^{-i\sigma \Omega_{i,-\sigma}}$. For the case of 1D hopping where $\theta_{ij} \in \{0, \pi\}$, this reduces to the transformation implemented in the main text. Note that in the one-hole case the above string operator can be further reduced to the form used in Refs. [28, 29].

2. Technical details on processing data with U(1) symmetry

The t - J model under uniform Zeeman field has both charge and spin U(1) symmetry so that the total spin S^z can only take integer values, which causes quantized m - h curves for finite-size systems shown in Fig. 2 of the main text. To take the derivative $\chi = \frac{\partial m}{\partial h}$ meaningfully, we smooth such quantized curves by connecting the midpoints of those quantized plateaus and performing finite-size scaling to obtain the onset and saturation of the magnetization. In addition, the legends in Fig. 3(a) and Fig. 4(d) results from keeping two decimals for $m = S^z/N$ with $S^z = 0, 4, 8, \dots, 36$ and $S^z = 0, 4, 8, \dots, 56$, respectively. The continuous Fourier spectrums in Figs. 2(c), (d), Figs. 3(b), (d) and (f) are obtained from the discrete spectrums at $S^z = 0, 4, 8, \dots, 56$ by the bicubic interpolation function.

3. Charge and spin density distributions

We provide typical real space distributions of charge and spin densities in Fig. S1 as complements of the Fourier spectrums shown in Figs. 2(c) and (d) of the main text, where the large uniform component $n(q=0)$ is artificially removed for better presentation. The charge and spin density distributions along the \hat{x} -direction are defined by

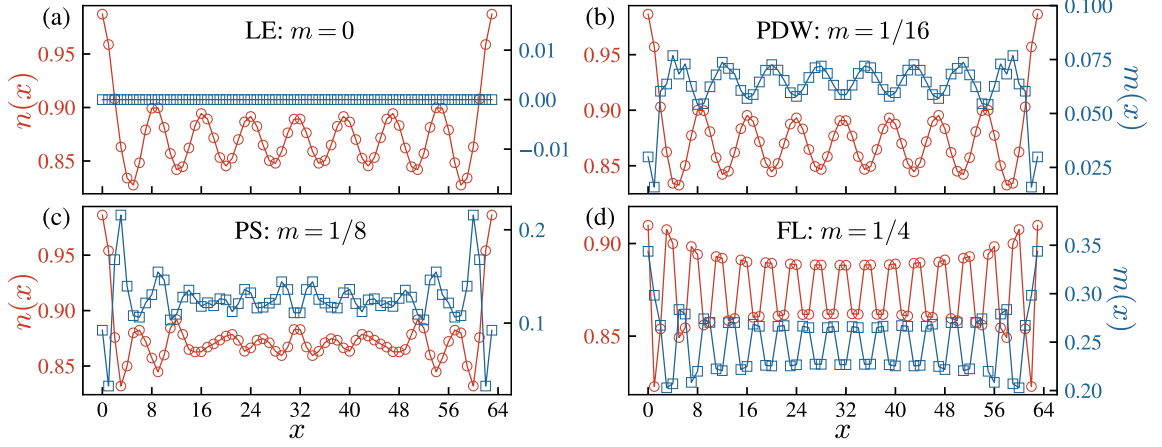


FIG. S1. Typical charge density profiles $n(x)$ and spin density profiles $m(x)$ of a two-leg t - J ladder with $\delta = 1/8$, $t_{\perp} = 3$ and lattice length $L_x = 64$ with respect to the four regions of the phase diagram in the main text.

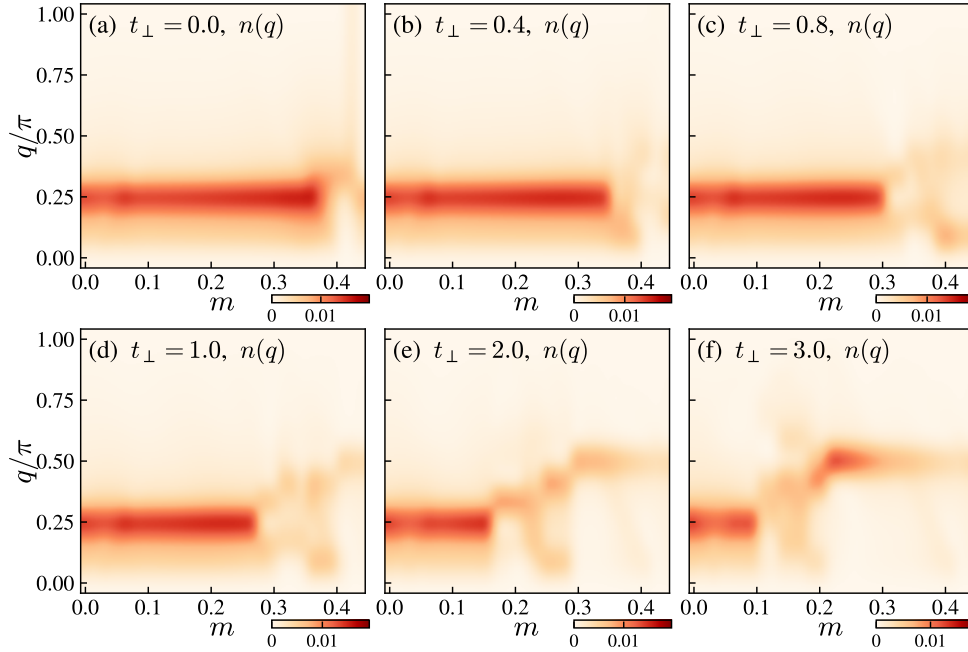


FIG. S2. Fourier spectrum $n(q)$ of charge density profile vs. the total magnetization m at different value of the interchain hopping integral t_{\perp} of a two-leg t - J ladder with doping $\delta = 1/8$ and lattice length $L_x = 32$.

$n(x) = \sum_y \langle n_{x,y} \rangle / L_y$ and $m(x) = \sum_y \langle S_{x,y}^z \rangle / L_y$, respectively. One can find that up to the boundary effect, the density profiles in the LE, PDW and FL phases have well-defined periodicities while those in the phase separation region are relatively irregular and inhomogeneous.

The main text contains the Fourier spectrum of charge density profile as a function of the magnetization at $t_{\perp} = 0$ and 3 of lattice length $L_x = 64$. We depict the same quantity at more values of t_{\perp} of length $L_x = 32$ in Fig. S2, where the discrete raw data at $S^z = 0, 1, 2, \dots, 28$ is interpolated. The Fourier spectrum is defined as $n(q) = |\sum_x n(x) e^{iqx}| / R$ where x is summed over the central bulk of length $R = 3L_x/4$ to reduce the boundary effect. The PDW, FL and phase separation regions together with their boundaries can be easily identified from the patterns of $n(q)$, i.e., a peak at $Q_{\text{CDW}} = 2\pi\delta$, a peak at $Q_{\text{CDW}} = 4\pi\delta$ and a relatively messy pattern with no predominant peak.

TABLE I. Estimation of typical power-law exponents or correlation lengths of the pair-pair correlator $P(r)$, the density-density correlator $D(r)$, the single-particle Green's function $G_\sigma(r)$ and the spin-spin correlator $F_\alpha(r)$. If the correlators decay algebraically $\sim r^{-K}$, we denote the corresponding power-law exponents as K_{sc} , K_c , K_G and K_s , respectively. Otherwise if they decay exponentially $\sim e^{-r/\xi}$, we denote the correlation lengths as ξ_{sc} , ξ_c , ξ_G and ξ_s .

Phase	$P(r)$	$D(r)$	$G_\sigma(r)$	$F_x(r)$	$F_z(r)$
LE	$K_{sc} \lesssim 1$	$1 < K_c < 2$	$\xi_G < 5$	$\xi_s < 7$	$\xi_s < 7$
PDW	$1 \lesssim K_{sc} \lesssim 2$	$K_c \lesssim 1$	$\xi_G < 7$	$K_s < 1$	$\xi_s < 7$
PS	$\xi_{sc} < 4$	$K_c < 2$	$K_G < 2$	$K_s < 1$	$K_s < 2$
FL	$\xi_{sc} < 4$	$K_c < 2$	$K_G < 2$	$K_s < 1$	$K_s < 2$

4. Other correlation functions

Fig. 3 depicts the pair-pair correlators of spin singlets $P(r)$, which can be represented as a summation of four elementary correlators

$$\begin{aligned}
\langle \Delta_{x_0}^\dagger \Delta_{x_0+r} \rangle &= \left\langle \frac{1}{2} \left(c_{x_0,2,\downarrow}^\dagger c_{x_0,1,\uparrow}^\dagger - c_{x_0,2,\uparrow}^\dagger c_{x_0,1,\downarrow}^\dagger \right) \left(c_{(x_0+r),1,\uparrow} c_{(x_0+r),2,\downarrow} - c_{(x_0+r),1,\downarrow} c_{(x_0+r),2,\uparrow} \right) \right\rangle \\
&= -\frac{1}{2} \left(\langle c_{x_0,1,\uparrow}^\dagger c_{x_0,2,\downarrow}^\dagger c_{(x_0+r),1,\uparrow} c_{(x_0+r),2,\downarrow} \rangle - \langle c_{x_0,1,\uparrow}^\dagger c_{x_0,2,\downarrow}^\dagger c_{(x_0+r),1,\downarrow} c_{(x_0+r),2,\uparrow} \rangle \right. \\
&\quad \left. - \langle c_{x_0,1,\downarrow}^\dagger c_{x_0,2,\uparrow}^\dagger c_{(x_0+r),1,\uparrow} c_{(x_0+r),2,\downarrow} \rangle + \langle c_{x_0,1,\downarrow}^\dagger c_{x_0,2,\uparrow}^\dagger c_{(x_0+r),1,\downarrow} c_{(x_0+r),2,\uparrow} \rangle \right). \tag{S5}
\end{aligned}$$

The overall negative sign before the $1/2$ factor is omitted in Fig. 3 by convention. We denote these elementary correlators as $P_{\sigma\sigma'}(r) = \langle c_{x_0,1,\sigma}^\dagger c_{x_0,2,-\sigma}^\dagger c_{(x_0+r),1,\sigma'} c_{(x_0+r),2,-\sigma'} \rangle$. The corresponding correlators of the pairing amplitude and phase can be defined similarly, i.e., $\tilde{P}_{\sigma\sigma'}(r) = \langle \tilde{c}_{x_0,1,\sigma}^\dagger \tilde{c}_{x_0,2,-\sigma}^\dagger \tilde{c}_{(x_0+r),1,\sigma'} \tilde{c}_{(x_0+r),2,-\sigma'} \rangle$ and $\Phi_{\sigma\sigma'}(r) = \langle e^{-i\phi_{x_0,\sigma}} e^{i\phi_{x_0+r,\sigma'}} \rangle$, where $\phi_{x,\sigma} = \Omega_{x1,-\sigma} + \Omega_{x2,\sigma}$. ($\phi_{x,\uparrow}$ is exactly the string-like operator ϕ_x in the main text.) To illustrate the composite structure of the pairing amplitude and phase more directly, we depict these elementary correlators in Fig. S3 on top of the summed correlators $P(r)$ in the main text. In consistent with the conclusions in the main text, one can find that $\tilde{P}_{\sigma\sigma'}(r)$ still exhibits no sign change and $\Phi_{\sigma\sigma'}(r)$ captures the PDW oscillation precisely.

Moreover, $\Phi_{\sigma\sigma}(r)$ and $\Phi_{\sigma,-\sigma}(r)$ [$P_{\sigma\sigma}(r)$ and $P_{\sigma,-\sigma}(r)$, $\tilde{P}_{\sigma\sigma}(r)$ and $\tilde{P}_{\sigma,-\sigma}(r)$] almost equal to each other [up to an overall negative sign], indicating that $\Phi(r)$ as a common factor can be extracted out from the summation in Eq. (S5). This explains why the summed correlator $P(r)$ also has a well-defined composite structure $P(r) \propto \tilde{P}(r)\Phi(r)$.

In addition, it is worth mentioning that in the LE and PDW phases, the overall magnitude of pair-pair correlator of spin singlets is notably higher than those of other spatial or spin configurations, e.g., bonds along the \hat{x} -direction, and spin triplets of both $S = 0$ and $S = 1$.

Finally, we provide the estimation of typical spatial decay behaviors of the pair-pair correlator together with other correlation functions in Table. I, including the density-density correlation function $D(r) = \frac{1}{L_y} \sum_{y=1}^{L_y} (\langle n_{x_0 y} n_{(x_0+r)y} \rangle - \langle n_{x_0 y} \rangle \langle n_{(x_0+r)y} \rangle)$, the single-particle Green's function $G_\sigma(r) = \frac{1}{L_y} \sum_{y=1}^{L_y} \langle c_{x_0 y, \sigma}^\dagger c_{(x_0+r)y, \sigma} \rangle$ and the spin-spin correlation function $F_\alpha(r) = \frac{1}{L_y} \sum_{y=1}^{L_y} (\langle S_{x_0 y, \alpha}^\alpha S_{(x_0+r)y, \sigma}^\alpha \rangle - \langle S_{x_0 y, \alpha}^\alpha \rangle \langle S_{(x_0+r)y, \sigma}^\alpha \rangle)$ where $\alpha \in \{x, y, z\}$ is the index of the spin component. One can see that $P(r)$ becomes short-ranged and $G_\sigma(r)$ becomes quasi-long-ranged from the LE and PDW regimes to the PS and FL regimes, in accordance with the results of the binding energy. $F_x(r)$ becomes quasi-long-ranged from the LE phase to the PDW phase, which further reveals the distinction between these two regimes.

5. The accurate separation of the pairing amplitude and phase at $t_\perp = 0$

We may further check the composite structure of the pairing order parameter in Eq. (4) of the main text by multiplying the correlators of $\tilde{P}_{\sigma\sigma'}(r)$ and $\Phi_{\sigma\sigma'}(r)$ in comparison with the original pair-pair correlator $P_{\sigma\sigma'}(r)$ in Fig. S4. One can find that up to an overall factor, the recombined $\tilde{P}_{\sigma\sigma'}(r) \times \Phi_{\sigma\sigma'}(r)$ coincides very precisely with $P_{\sigma\sigma'}(r)$, which confirms that the pairing amplitude and phase can be well described by $\langle \tilde{c}_{x1,\uparrow} \tilde{c}_{x2,\downarrow} \rangle$ and $\langle e^{i\phi_x} \rangle$ respectively, i.e., $\langle c_{x1,\uparrow} c_{x2,\downarrow} \rangle = \langle \tilde{c}_{x1,\uparrow} \tilde{c}_{x2,\downarrow} e^{i\phi_x} \rangle \propto \langle \tilde{c}_{x1,\uparrow} \tilde{c}_{x2,\downarrow} \rangle \langle e^{i\phi_x} \rangle$ as a generalized mean-field-type separation (with an appropriately determined overall renormalization factor).

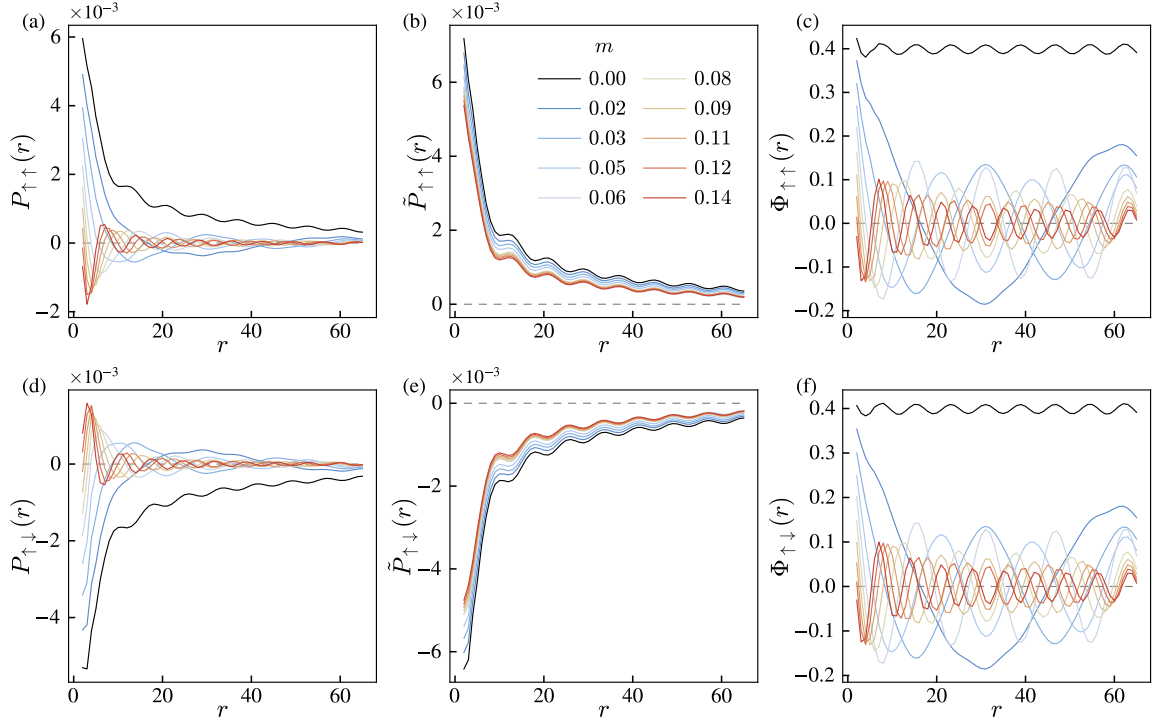


FIG. S3. Four elementary correlators $P_{\sigma\sigma'}(r)$ constituting the pair-pair correlator of spin-singlets $P(r)$, together with the corresponding correlators of the twisted pairs $\tilde{P}_{\sigma\sigma'}(r)$ and the twisting phase $\Phi_{\sigma\sigma'}(r)$. These correlators are measured on a two-leg t - J ladder with $t_{\perp} = 0$, $\delta = 1/8$ and $L_x = 128$ at different magnetizations m . Only $P_{\uparrow\uparrow}(r)$ and $P_{\uparrow\downarrow}(r)$ are depicted since $P_{\sigma\sigma'}(r)$ and $P_{-\sigma,-\sigma'}(r)$ are equivalent under the reflection symmetry between the two chains of the two-leg ladder.

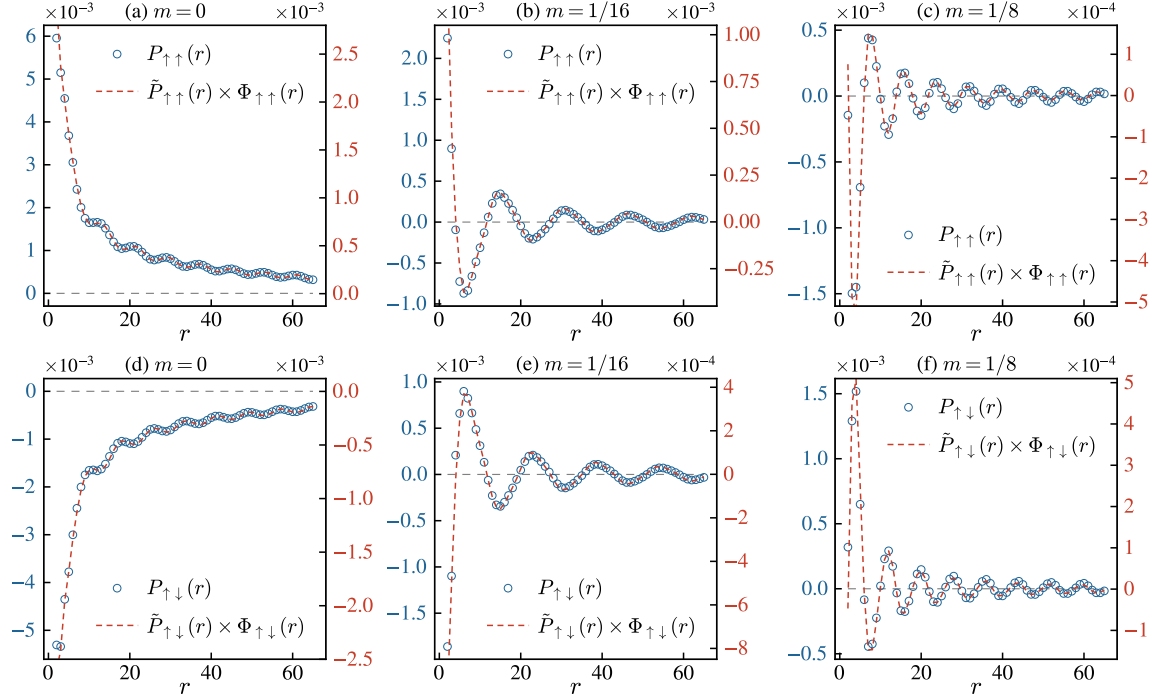


FIG. S4. Recombining $\tilde{P}_{\sigma\sigma'}(r)$ and $\Phi_{\sigma\sigma'}(r)$ can reproduce $P_{\sigma\sigma'}(r)$ very accurately except for an overall factor. These correlators are measured on a two-leg t - J ladder with $t_{\perp} = 0$, $\delta = 1/8$ and $L_x = 128$.